Universal Journal of Renewable Energy **1 (2013), 1-22**
www.papersciences.com

Non-linear Singular Integral Computational Method for Wind Energy

E.G. Ladopoulos
Interpaper Research Organization
8, Dimaki Str.
Athens, GR - 106 72, Greece
eladopoulos@interpaper.org

Abstract
By using the field theory of Green, the general problem of the unsteady flow of a two-dimensional NACA airfoil is reduced to the solution of a non-linear multidimensional singular integral equation. This nonlinearity results from the fact that the source and vortex strength distributions, are dependent on the history of the vorticity and source distribution on the NACA airfoil surface. Applications are given to the determination of the velocity field around the blades of a vertical axis wind turbine for four special cases: 1) constant source distribution. 2) linear source distribution. 3) constant vortex distribution. 4) linear vortex distribution. The vertical axis wind turbines have a continuously increasing aspect, for the minimization of the cost per unit produced energy. By this type of very large wind turbines (with diameters up to 200m and power outputs up to 20 MW) will be covered a big percentage of the energy consumption world-wide.

Key Word and Phrases
Non-linear Singular Integral Equations, Unsteady Flow, Wind Energy, Vertical Axis Wind Turbines, NACA airfoil, Source Distribution, Vortex Distribution.

1. Present Status of Wind Energy – Future Applications

The fundamental purpose of this investigation is to explore the scientific and engineering problems involved to the design of wind energy conversion systems. At the time of writing the present research, there is universal anxiety about the Green-house Effect and the acid rain caused by the burning of oil, natural gas and coal. In the post – Chernobyl era, the nuclear solution is also facing severe environmental obstacles. In the meantime, thousands of megawatts of wind turbines have been installed in Californian wind farms and thousands more are planned for European wind farms in the next years. Although such contributions do not represent a very large part of the world's electricity supply at present, they are growing and wind may well become a major source of power over the next years.

Wind result from the fact that the Earth's equatorial regions receive more solar energy than the polar regions, and this sets up large – scale convection currents in the atmosphere. Meteorologists estimate that about 1% of the incoming solar radiation is converted to wind energy. Since the solar energy received by the Earth in just ten days has an energy content equal to the world's entire fossil fuel reserves (coal, oil and gas), this means that the wind resource is extremely large.

One percent of the daily wind energy input (i.e. 0.01% of the incoming solar energy) is equivalent to the present world daily energy consumption. Although global resource estimates have relevance, more detailed assessments are required to quantify the resource in a particular area. A detailed study performed recently under the auspices of the EU and involving specialists in all the EU countries, concluded that there were suitable sites within the EU for 400.000 MW scale wind turbines, which would be able to provide 4000 TWh of electricity per year. This is approximately three times Europe's present electricity consumption and corresponds to an inexhaustible output of about 16 million barrels per day (m.b.d.). Europe's wind energy resources is therefore a major one.

Winds are only an intermittent source of energy, day by day, though they represent a reliable energy source year by year. It is now clear that the major applications of wind energy will involve electricity generation, with the wind turbines operating in parallel with utility grid systems or – in more remote locations – in parallel with diesel engines. The wind turbines role is to reduce fossil fuel consumption and to reduce overall electricity generation costs. Utilities have the flexibility to

accept a contribution of about 20% from wind energy systems at present and potentially substantially more. Wind-diesel systems can be designed to provide more than 50% fuel saving.

A modern wind turbine efficiently intercepts the wind energy flowing through the entire rotor swept area even though it has only two or three blades, with a solidity (equals the blade area/rotor swept area) in the range of 5 to 10%. This low solidity means that the wind turbine is an effective energy concentrator, with power densities per unit blade area of about 1000 W/m^2, and as a result the energy recovery period of the turbine is relatively short, i.e. about one year. This means that the wind turbine will repay the energy invested in its construction within about one year of operation. Though the applications of wind energy systems depend primarily on their economic competitiveness, their short energy recovery period is an encouraging pointer towards their economical potential.

Particularly notable has been the wind energy program initiated by the U.S.A. after the 1973 oil crisis, whose first visible result was the installation in 1975, near Cleveland, Ohio, of the Mod. O wind turbine, a 38m diameter two-bladed horizontal axis machine with a rated power output of 100 KW. The subsequent development of large wind turbines in the U.S.A. led to the completion in 1981 of the 91 diameter, 2.5 MW rated, Boeing Mod. 2 wind turbine. Five of these large wind turbines were completed, and three of them were installed at Goldendale, in the state of Washington.

A number of other multi – megawatt wind turbines have also been completed since 1980, including two built by Hamilton-Standard (U.S.A.) in cooperation with a Swedish company, Wind Turbine Systems. Both were completed in 1982, the 3 MW WTS3 in Sweden and the 4 MW WTS4 in the U.S.A., and have since been undergoing test and evaluation. In California in the early 1980's, the combination of high wind speeds (in certain east-west mountain passes) and renewable energy tax incentives permitted the rapid development of privately-financed wind farms and by early 1987 approximately 1500 MW of wind turbine capacity was provided by about 1500 wind turbines, mostly with diameters in the range of 15 to 25 m.

Encouraged by developments in California, wind farms have since been installed in Denmark, Germany, Spain, U.K., Netherlands and the Greek islands and many more countries have plans to install them. By comparison with most existing methods of producing electricity, wind turbines are environmentally benign and many more countries see the use of wind energy as a means of reducing their dependence on imported fuels.

Worldwide, the cost of electricity from wind turbines will depend on the magnitude of local wind speeds and their competitiveness will also depend on the costs of electricity from existing sources (e.g. low-cost hydro or high-cost oil). However it is now clear that wind energy systems will be used worldwide in very large numbers over the next years. The past decade has been one of rapid development and has seen the beginnings of the large-scale use of wind energy systems. The current decade promise a very much increase.

Our proposals for investigation concerns mainly to the design of the vertical axis wind turbines. The main attractions of this design are that this class of wind turbine is omnidirectional and the vertical drive shaft simplifies the installation of the gearbox and generator. Vertical axis wind turbine proponents believe that this type of wind turbine can be made substantially larger than horizontal axis machines and one of the objectives of the U.K. vertical axis wind turbine program is to develop multi-megawatt machines suitable for offshore use. Offshore wind speeds are high and the visual impact associated with deploying large numbers of wind turbines is minimized if these are cited many kilometers offshore. Some studies have shown that offshore wind energy systems could provide a substantial fraction of electricity requirements.

It is therefore believed that now is the proper time to develop very large vertical axis wind turbines (with diameters up to 200 m and power outputs up to 20 MW) and by these will be covered a big percentage of the energy consumption within the E.U. Our proposal for investigation concerns therefore to the study of a very modern computational method which will be used for the design of such very large vertical axis wind turbines. In the next sections will be outlined the analytical theory of the proposed computational method.

2. Non-linear Singular Integral Computational Method

2.1 Introduction

Over the last years, the non-linear singular integral equations developed an increasing interest, because of their application to the solution of general problems of the fluid mechanics theory, referring to unsteady flows. Such fluid mechanics and aerodynamic problems, are reduced to the solution of a non-linear singular integral equation, connected with the design and evaluation of the aerodynamic characteristics of an airfoil section.

These aerodynamic characteristics of the NACA airfoils were always an important element in several engineering designs, like aircraft wings, turbo-machinery vanes, helicopter rotors, propellers and prop fans. Recently, the continuous improvement of the wind turbines structures, for the minimization of the cost per unit produced electric energy, has concentrated the attention on aerodynamic applications connected with wind energy methods.

Several linear singular integral equation methods of the finite-part and multidimensional type were investigated and improved during the recent years by E.G.Ladopoulos [1] – [17] and E.G.Ladopoulos et al [18] – [23] for the solution of elasticity, plasticity, aerodynamics and fracture mechanics problems. Beyond the above, E.G.Ladopoulos [24], [25] extended his theory to the solution of some non-linear integro-differential equations applied to solid mechanics problems.

Furthermore, E.G.Ladopoulos and V.A.Zisis [26], [27] used the non-linear singular integral equation method for the solution of two-dimensional fluid mechanics problems and E.G.Ladopoulos [28], [29} for the investigation of inviscid flow-fields of unsteady airfoils. Also, an approximation method for the solution of the non-linear singular integral equations was proposed by E.G.Ladopoulos and V.A.Zisis [30].

On the other hand, A.M.O.Smith and J.L.Hess [31], were the first scientists who investigated aerodynamic panel methods for studying airfoils with zero lift, while they modeled the airfoil either distributed potential source panels for nonlifting flows, or with vortex panels for flow with lift. Their method was extended to three-dimensional steady and unsteady flows, by combining source and vortex singularities, by R.H.Djojodihardjo and S.E.Widnall [32], P.E.Robert and G.A.Saaris [33], J.M.Summa [34], T.Sapkaya and R.L.Schoaff [35], D.R.Bristow [36] and J.D.Hawk [37] and R.I.Lewis [38].

Potential flow models for airfoil investigations, were introduced by N.D.Ham [39], F.D.Deffenbaugh and F.J.Marschall [40], M.Kiya and M.Arie [41], and T.Sarpkaya and H.K.Kline [42], while the separating boundary layers were represented by an array of discrete vortices.

Beyond the above, over the last years some extensive investigations were done by R.E.Singleton and J.F.Nash [43], J.F.Nash, L.W.Carr and R.E.Singleton [44], A.A.Lyrio, J.H.Ferzinger and S.J.Kline [45], J.Kim, S.J.Kline and J.P.Johnston [46] and W.J.McCroskey and S.I.Pucci [47], by using unsteady turbulent boundary layer methods.

A continuously increasing interest during the recent years, on the wind turbines for energy applications, has concentrated the research to the studies of aerodynamic applications in connection with wind energy methods. The vertical axis wind turbines have a continuously increasing aspect, for the minimization of the cost per unit produced electric energy.

For studying vertical axis wind turbines, R.J.Muraca, M.V.Stephens and J.R.Dagenhart [48], J.H.Strickland [49], P.N. Shankar [50] and R.E.Wilson, P.B.S.Lissaman and S.N.Walker [51] have introduced a momentum model, consisting on the use of multiple streamtubes. This model was improved by I.Paraschivoiu [52], I.Paraschivoiu et al [53] and J.L.Loth and McCoy [54] by proposing a method, by separating the flow in two different parts.

Furthermore, a vortex method was also introduced, for the study of vertical axis wind turbines, by J.B.Fanucci and R.E.Walters [55] and J.H.Strickland, B.T. Webster and T.Nguyen [56], [57], while the last authors extended their model to three-dimensional, too.

In the present investigation, by using the field theory of Green, the general problem of the unsteady flow of a 2-dimansional NACA airfoil is reduced to the solution of a non-linear multidimensional singular integral equation. This nonlinearity results from the fact that the source

and vortex strength distributions, are dependent on the history of the vorticity and source distribution on the NACA airfoil surface.

Applications are given to the determination of the velocity field around the blades of a vertical axis wind turbine for four special cases: 1) constant source distribution 2) linear source distribution 3) constant vortex distribution and 4) linear vortex distribution.

2.2 Non-linear Unsteady Fluid Mechanics Representation

Consider a two-dimensional airfoil moving in an homogeneous, incompressible and inviscid fluid. (Fig.1).

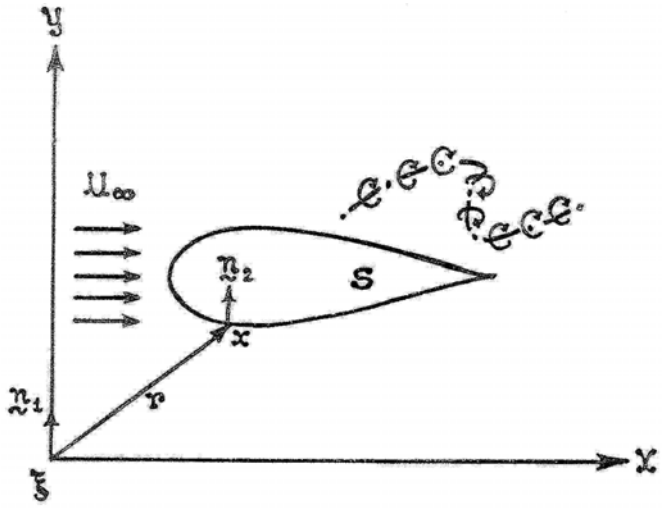

Fig. 1 A two-dimensional airfoil of surface S in an homogeneous, incompressible and inviscid fluid.

The airfoil with the wake comprise a complete lifting system in an irrotational flow through the ideal fluid. Because of this irrotationality, then for the local fluid velocity $\mathbf{U}$ we have:

$$\nabla \times \mathbf{U} = 0 \tag{2.2.1}$$

By replacing the fluid velocity with the total velocity potential H one obtains:

$$\mathbf{U} = \nabla H \tag{2.2.2}$$

while (2.2.2) can be further written as:

$$\mathbf{U} = \mathbf{U}_{\infty} + \nabla h \tag{2.2.3}$$

with $\mathbf{U}_{\infty}$ the outward velocity (Fig.1) and h the potential due to the presence of the airfoil.

Because of the conservation of mass for an incompressible fluid, the vector field doesn't diverge:

$$\nabla \cdot \mathbf{U} = 0 \tag{2.2.4}$$

By using (2.2.2), (2.2.3) and (2.2.4) we obtain equation of Laplace which is the governing equation:

$$\nabla^2 h = 0 \tag{2.2.5}$$

Moreover, the use of Green's theorem [58] results the following relation for the velocity potential $h(\mathbf{x},t)$, with t the time, at any point $\mathbf{x}$ in continuous, acyclic irrotational flow:

$$h(\mathbf{x},t) = -1/2\pi \int_S \frac{\omega[\xi,t,h]}{r} \mathrm{d}S + 1/2\pi \int_{S+W} \delta[\xi,t,h] \frac{\partial}{\partial n_1}\left(\frac{1}{r}\right) \mathrm{d}S \tag{2.2.6}$$

with S the surface of the airfoil (Fig.1), W the surface of the wake, $\mathbf{n_1}$ the surface normal at the source point ξ (Fig.1), $\omega[\xi,t,h]$ the source strength distribution, $\delta[\xi,t,h]$ the vortex strength distribution and r the distance equal to:

$$r = |\mathbf{x} - \xi| \tag{2.2.7}$$

Moreover, (2.2.6) can be written as following, which denotes a two-dimensional non-linear singular integral equation:

$$h(\mathbf{x},t) = -1/2\pi \int_S \frac{\omega[\xi,t,h]}{r} \mathrm{d}S + 1/2\pi \int_{S+W} \frac{\delta[\xi,t,h]}{r^2} \mathrm{d}S \tag{2.2.8}$$

The kinematical surface tangency condition on the surface of the airfoil has to be valid: [59]

$$\left(1/|\nabla S(\mathbf{x},t)|\right) \frac{\partial S(\mathbf{x},t)}{\partial t} + \frac{\partial h}{\partial n_2} + \mathbf{U}_\infty \cdot \mathbf{n}_2 = 0 \tag{2.2.9}$$

where $\mathbf{n}_2$ denotes the surface normal at the field point $\mathbf{x}$ (Fig.1).

This condition can be also written in the following form, for a body fixed coordinate system:

$$\left(1/|\nabla S(\mathbf{x},t)|\right) \frac{\partial S(\mathbf{x},t)}{\partial t} = -\left(\mathbf{U}_A + \boldsymbol{\omega}_\mathbf{A} \times \mathbf{x}\right) \cdot \mathbf{n}_2 \tag{2.2.10}$$

in which $\mathbf{U}_A$ denotes the airfoil translation velocity and $\boldsymbol{\omega}_\mathbf{A}$ the airfoil angular rotation.

From (2.2.9) and (2.2.10) follows:

$$\frac{\partial h}{\partial n_2} + \left(\mathbf{U}_\infty - \mathbf{U}_A - \boldsymbol{\omega}_A \times \mathbf{x}\right) \cdot \mathbf{n}_2 = 0 \tag{2.2.11}$$

Hence, by inserting (2.2.11) into (2.2.8) results the following two-dimensional non-linear singular integral equation:

$$\begin{gathered} 1/2\pi \int_S \omega[\xi,t,h] \frac{\partial}{\partial n_2}\left(\frac{1}{r}\right) \mathrm{d}S + 1/2\pi \int_{S+W} \delta[\xi,t,h] \frac{\partial}{\partial n_2}\left(\frac{1}{r^2}\right) \mathrm{d}S = \\ -\left(\mathbf{U}_\infty - \mathbf{U}_A - \boldsymbol{\omega}_A \times \mathbf{x}\right) \cdot \mathbf{n}_2 \end{gathered} \tag{2.2.12}$$

The non-linear singular integral equation (2.2.12) can be further written as:

$$1/2\pi \int_S \frac{\omega[\xi,t,h]}{r^2} \mathrm{d}S + 1/\pi \int_{S+W} \frac{\delta[\xi,t,h]}{r^3} \mathrm{d}S = \left(\mathbf{U}_\infty - \mathbf{U}_A - \boldsymbol{\omega}_\mathbf{A} \times \mathbf{x}\right) \cdot \mathbf{n_2} \tag{2.2.13}$$

Hence, by solving the non-linear singular integral equation (2.2.13) with the corresponding boundary conditions, then the velocity at any field point will be determined through (2.2.8).

2.3 Non-linear airloads analysis

The pressure distribution on the airfoil will be determined by the unsteady Bernoulli equation, valid at any point in an irrotational, ideal flow:

$$P = P_\infty - \rho\left[\frac{\partial H}{\partial t} + 1/2\left(\nabla H\right)^2\right] \tag{2.3.1}$$

where ρ is the fluid density.

By using the derivation of the previous section, then (2.3.1) may be written as:

$$P = P_\infty - \rho\left[\frac{\partial h}{\partial t} + \left(\mathbf{U}_\infty - \mathbf{U}_A - \boldsymbol{\omega}_A \times \mathbf{x}\right) \cdot \nabla h + 1/2\left(\nabla h\right)^2\right] \tag{2.3.2}$$

Moreover, (2.3.2) takes the following form:

$$P = P_\infty - \rho\left[\frac{\partial H}{\partial t} + \left(\mathbf{U}_\infty - \mathbf{U}_A - \boldsymbol{\omega}_A \times \mathbf{x}\right) \cdot \nabla_S H + \right.$$
$$\left. + \frac{\partial H}{\partial n_1}\left(\mathbf{U}_\infty - \mathbf{U}_A - \boldsymbol{\omega}_A \times \mathbf{x}\right) \cdot \mathbf{n}_1 + 1/2\left(\nabla_S H\right)^2 + 1/2\left(\frac{\partial H}{\partial n_1}\right)^2\right] \tag{2.3.3}$$

by replacing the ∇h, by the surface gradient $\nabla_S h$:

$$\nabla h = \nabla_S h + \frac{\partial h}{\partial n_1} \varepsilon_{n_1} \tag{2.3.4}$$

Because of (2.2.11), then (2.3.3) takes the form:

$$P = P_\infty - \rho\left[\frac{\partial H}{\partial t} + \left(\mathbf{U}_\infty - \mathbf{U}_A - \boldsymbol{\omega}_A \times \mathbf{x}\right) \cdot \nabla_S H - \right.$$
$$\left. - 1/2\left\{\left(\mathbf{U}_\infty - \mathbf{U}_A - \boldsymbol{\omega}_A \times \mathbf{x}\right) \cdot \mathbf{n}_1\right\}^2 + 1/2\left(\nabla_S H\right)^2\right] \tag{2.3.5}$$

which will be used for the computation.

2.4 Velocity Calculations for Constant Source Distribution

Consider the special case of a constant source distribution ω. In this case the general non-linear problem presented in the previous sections is much more simplified and is solved as a linear

problem. The geometrical representation of the problem is shown in Fig. 2.

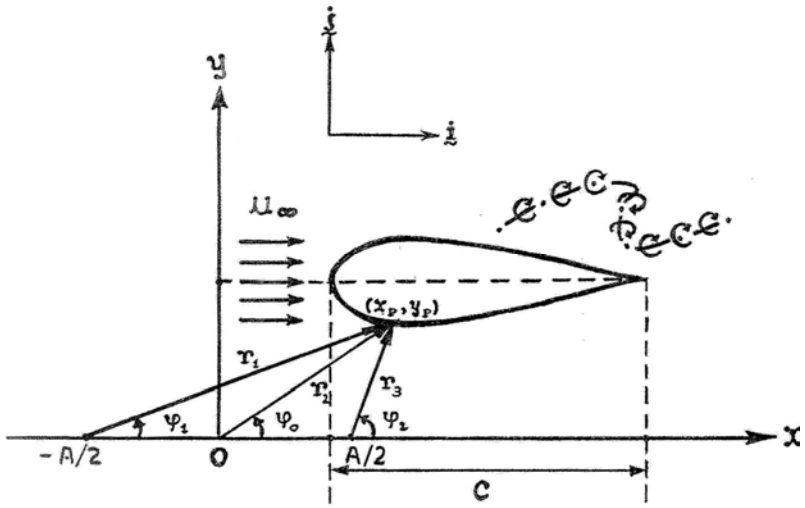

Fig. 2 Coordinate system for the two-dimensional airfoil.

In this case the fluid velocity $\mathbf{U}$ is calculated as following:

$$\mathbf{U} = \int_{-A/2}^{A/2} \frac{\omega \, \mathrm{d}\, r}{2\pi r} \left(\cos\varphi \mathbf{i} + \sin\varphi \mathbf{j} \right) \tag{2.4.1}$$

where $\mathbf{i}$, $\mathbf{j}$ are the unit vectors on the x and y axis, respectively, and A denotes the separating wake. (Fig. 2).

Hence, the fluid velocity $\mathbf{U}$ can be determined as following, for the cases when $y_p \neq 0$ and $y_p = 0$:

$$\mathbf{U} = \begin{cases} \omega/2\pi \left[\ln\left|\dfrac{r_1}{r_2}\right| \mathbf{i} - (\varphi_1 - \varphi_2)\mathbf{j} \right], & y_p \neq 0 \\ \omega/2\pi \ln\left|\dfrac{r_1}{r_2}\right| \mathbf{i}, & y_p = 0 \end{cases} \tag{2.4.2}$$

Moreover, consider the pressure coefficient C_p:

$$C_p = (P - P_\infty)/(1/2\, \rho U_\infty^2) \tag{2.4.3}$$

where ρ denotes the fluid density and P_∞ the stream pressure.

By using Bernoulli's equation, then the coefficient C_p may be written as:

$$C_p = -U^2/U_\infty^2 \tag{2.4.4}$$

which can be used for the calculations.

2.5 Velocity Calculations for Linear Source Distribution

By considering the special case of a linear source distribution ω, then the general non-linear problem, studied is much more simplified and is solved as a linear problem. In this case, we study two different approaches of the problem: the first when the linear source distribution is presented in the left-hand side of the separating wake and the second when presented in the right-hand side of the wake. The geometrical representation of this problem is shown again in Fig. 2.

By supposing linear source distribution in the left-hand side of the separating wake, then the fluid velocity $\mathbf{U}_L$ is determined as following:

$$\mathbf{U}_L = \int_{-A/2}^{0} \frac{\omega dr}{2\pi r}\left(\cos\varphi\mathbf{i} + \sin\varphi\mathbf{j}\right) \tag{2.5.1}$$

in which A denotes the separating wake (Fig. 2) and $\mathbf{i}$ and $\mathbf{j}$ are the unit vectors on the x and y axes, respectively.

Therefore, for the cases where $y_p \neq 0$ and $y_p = 0$, then the fluid velocity U_L will be computed as following:

$$\mathbf{U}_L = \begin{cases} a/2\pi\left[x_p \ln\left|\dfrac{r_1}{r_2}\right| - A/2 + y_p(\varphi_0 - \varphi_1)\right]\mathbf{i} \\ -a/2\pi\left[x_p(\varphi_1 - \varphi_0) + y_p \ln\left|\dfrac{r_1}{r_2}\right|\right]\mathbf{j}, \quad y_p \neq 0 \\ a/2\pi\left[x_p \ln\left|\dfrac{r_1}{r_2}\right| - A/2\right]\mathbf{i}, \qquad y_p = 0 \end{cases} \tag{2.5.2}$$

where a is the angle of attack.

On the other hand, by supposing right-hand source distribution in the right hand side of the separating wake, then the fluid velocity $\mathbf{U}_R$ is determined by the following integral:

$$\mathbf{U}_R = \int_{0}^{A/2} \frac{\omega\,\mathrm{d}\,r}{2\pi r}(\cos\varphi\mathbf{i} + \sin\varphi\mathbf{j}) \tag{2.5.3}$$

Hence, the fluid velocity $\mathbf{U}_R$ will be computed as following, for the cases where $y_p \neq 0$ and $y_p = 0$:

$$\mathbf{U}_R = \begin{cases} a/2\pi\left[x_p \ln\left|\dfrac{r_1}{r_2}\right| - A/2 + y_p(\varphi_2 - \varphi_0)\right]\mathbf{i} \\ -a/2\pi\left[x_p(\varphi_0 - \varphi_2) + y_p \ln\left|\dfrac{r_1}{r_2}\right|\right]\mathbf{j}, \quad y_p \neq 0 \\ a/2\pi\left[x_p \ln\left|\dfrac{r_1}{r_2}\right| - A/2\right]\mathbf{i}, \qquad y_p = 0 \end{cases} \tag{2.5.4}$$

For the numerical evaluation of the pressure coefficient will be used (2.4.4), as for the previous case.

2.6 Velocity Calculations for Constant Vortex Distribution

Consider the special case of a constant vortex distribution λ. Then, the non-linear problem is again simplified and is solved as a linear problem. The geometrical representation of this problem is shown in Fig.2.

For constant vortex distribution λ, then the fluid velocity $\mathbf{U}$, is determined by the formula:

$$\mathbf{U} = \int_{-A/2}^{A/2} \frac{\lambda \, \mathrm{d}\, r}{2\pi r} \left(-\sin\varphi \mathbf{i} + \cos\varphi \mathbf{j} \right) \tag{2.6.1}$$

where A is the separating wake (Fig. 2) and $\mathbf{i}, \mathbf{j}$ are the unit vectors on the x and y axis, respectively.

Hence, when $y_p \neq 0$ and $y_p = 0$, then the fluid velocity $\mathbf{U}$ will be computed as following:

$$\mathbf{U} = \begin{cases} \lambda/2\pi \left[(\varphi_1 - \varphi_2)\mathbf{i} + \ln\left|\frac{r_1}{r_2}\right| \mathbf{j} \right], & y_p \neq 0 \\ \lambda/2\pi \ln\left|\frac{r_1}{r_2}\right| \mathbf{j}, & y_p = 0 \end{cases} \tag{2.6.2}$$

For the numerical computations of the pressure coefficient will be used again (2.4.4), as for the previous cases.

2.7 Velocity Calculations for Linear Vortex Distribution

Suppose the special case of a linear vortex distribution δ. In this case the general non-linear problem will be again much more simplified and will be solved as a linear problem. The geometrical representation of this problem is again shown in Fig. 2.

For a linear vortex distribution δ, then the fluid velocity $\mathbf{U}$ is given as following:

$$\mathbf{U} = \int_{-A/2}^{A/2} \frac{\delta \, \mathrm{d}\, r}{2\pi r} \left(-\sin\varphi \mathbf{i} + \cos\varphi \mathbf{j} \right) \tag{2.7.1}$$

where A denotes the separating wake (Fig. 2) and $\mathbf{i}, \mathbf{j}$ the unit vectors in the x and y axis, respectively.

Hence, the fluid velocity $\mathbf{U}$ will be computed through the following relations, for the cases when $y_p \neq 0$ and $y_p = 0$:

$$\mathbf{U}=\begin{cases} a/2\pi\left[x_p(\varphi_1-\varphi_2)+y_p\ln\left|\frac{r_1}{r_2}\right|\right]\mathbf{i}+a/2\pi\left[x_p\ln\left|\frac{r_1}{r_2}\right|-A-y_p(\varphi_1-\varphi_2)\right]\mathbf{j}, & y_p\neq 0 \\ a/2\pi\left[x_p\ln\left|\frac{r_1}{r_2}\right|-A\right]\mathbf{j}, & y_p=0 \end{cases} \tag{2.7.2}$$

where a is the angle of attack.

For the numerical evaluation of the pressure coefficient will be used again (2.4.4), as for the previous three special cases.

2.8 Vertical Axis Wind Turbine Linear Applications

The previous mentioned two-dimensional fluid mechanics analysis, will be used for the calculation of the velocity field presented in a vertical axis wind turbine. A computer program was therefore written by using Visual Basic. This computer program presents the four linear cases described in sections 2.4 to 2.7.

As an example, the geometrical sizes of the vertical axis wind turbine considered are: Head diameter: $D=1.60m$, length: $H=1.10m$, 2 blades, blade chord: $c=0.12m$ and blade airfoil section NACA 0018 (Fig. 3).

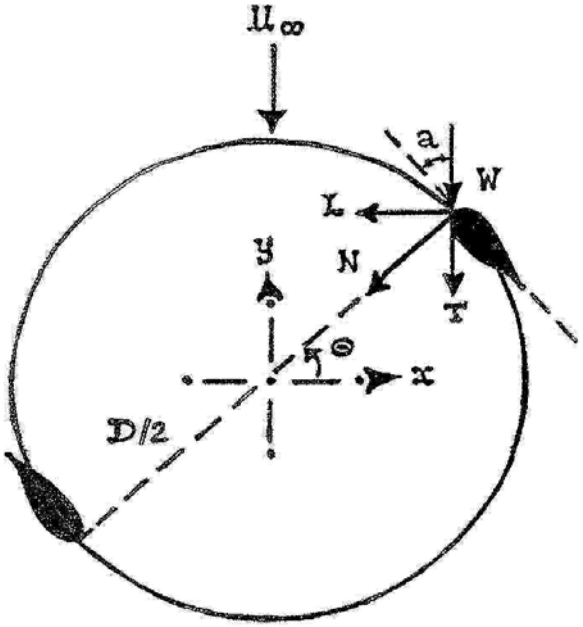

Fig. 3 Arrangement of a vertical axis wind turbine.

Firstly, by supposing unit source distribution, the velocity field on the boundary of the airfoil was computed by (2.4.2) for azimuthal angle $\Theta=90°$. Also, the pressure coefficient C_p was calculated by (2.4.4) for several wind velocities U_∞. Therefore, Figures 4,5,6 and 7 show the pressure distribution on the vertical axis wind turbine presented, for wind speed $U_\infty=10,15,20,25m/s$, respectively.

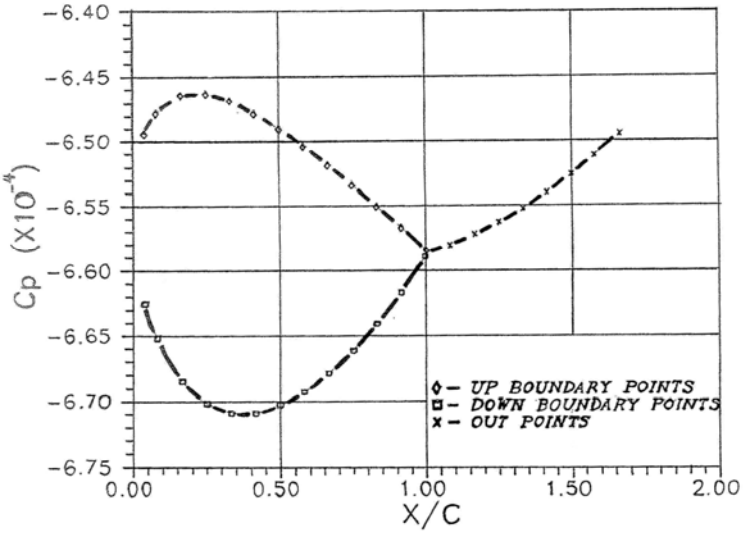

Fig. 4 Pressure distribution on the vertical axis wind turbine of Fig.3, for unit source distribution and wind speed 10 m/sec.

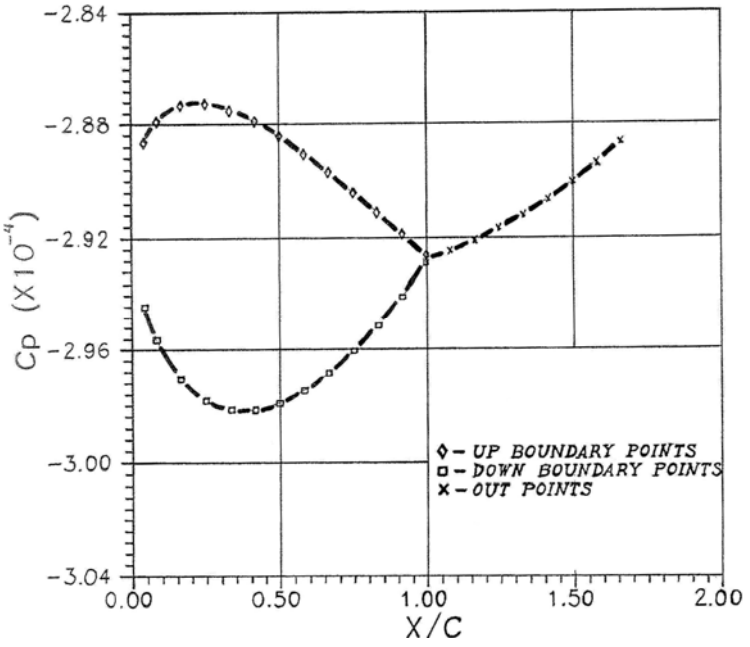

Fig. 5 Pressure distribution on the vertical axis wind turbine of Fig.3, for unit source distribution and wind speed 15 m/sec.

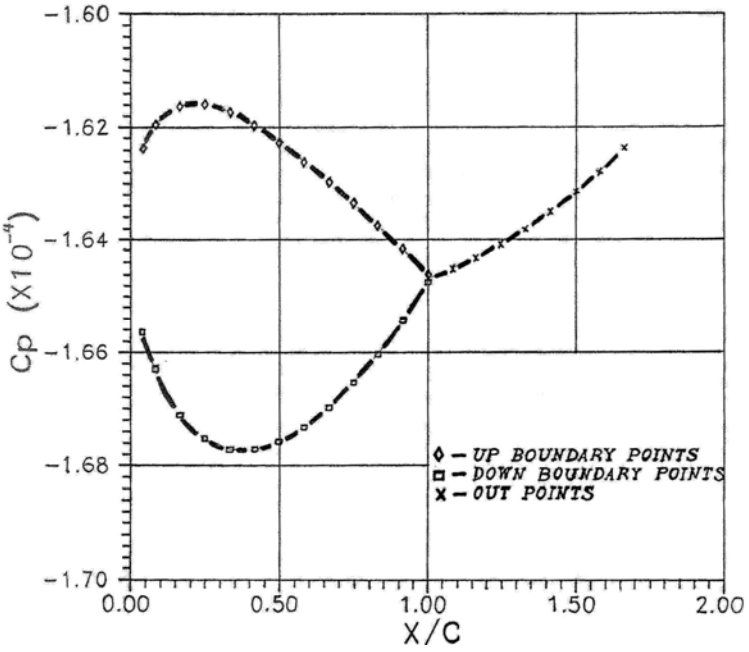

Fig. 6 Pressure distribution on the vertical axis wind turbine of Fig.3, for unit source distribution and wind speed 20 m/sec.

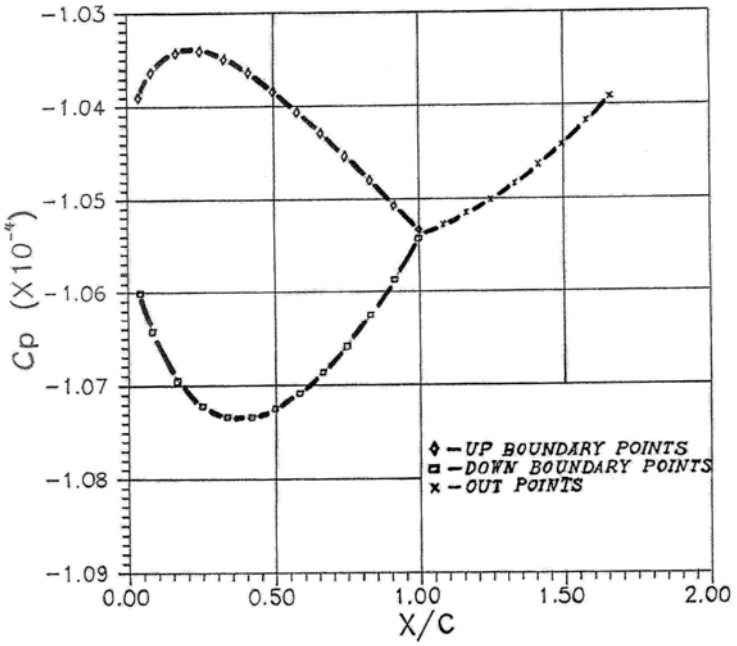

Fig. 7 Pressure distribution on the vertical axis wind turbine of Fig.3, for unit source distribution and wind speed 25 m/sec.

By these Figures it is shown, that for the up boundary points of the airfoil the values of the pressure coefficient are increasing approximately, up to $x/c = 0.25$, while they are decreasing again to $x/c = 1$. On the other hand, for the down boundary points the values of C_p are decreasing up to $x/c = 0.35$, and then increasing up to $x/c = 1$.

Secondly, by supposing linear source distribution in the left-hand or in the right-hand of the separating wake, the velocity field on the boundary and outside of the airfoil was computed by (2.5.2) for the left-hand side and by (2.5.4) for the right-hand side, for both cases for azimuthal angle $\Theta = 90°$. Moreover, the pressure coefficients C_p were computed for both cases through (2.4.4), for several wind velocities U_∞ and it was supposed angle of attack $a = 20°$.

Hence, Figures 8 and 9 show the pressure distribution on the vertical axis wind turbine presented, for linear source distribution in the left side of the separating wake and for wind speed $U_\infty = 10 \text{ and } 15 m/s$, respectively.

On the other hand, Figures 10 and 11 show the pressure distribution on the vertical axis wind turbine, for a linear source distribution in the right-hand side of the separating wake and for wind speed $U_\infty = 10 \text{ and } 15 m/s$, respectively.

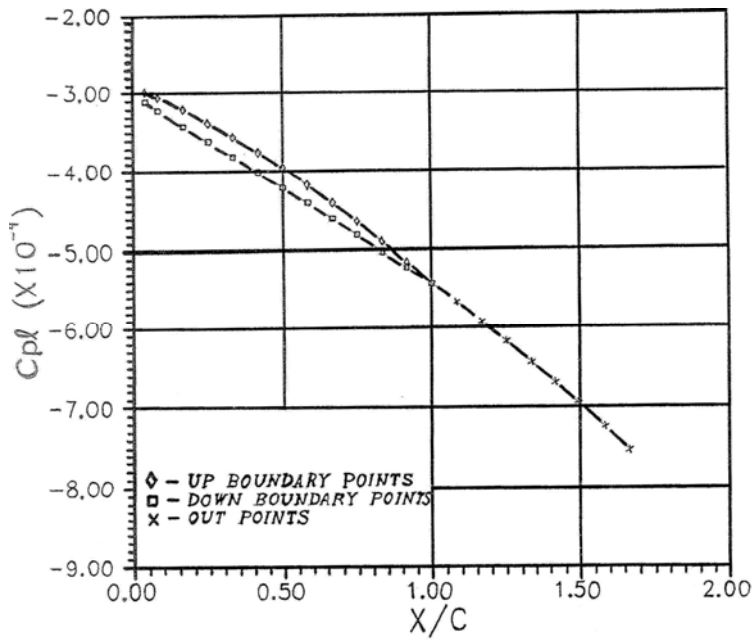

Fig. 8 Pressure distribution on the vertical axis wind turbine of Fig.3, for linear source distribution in the left side of the separating wake and for wind speed 10 m/sec.

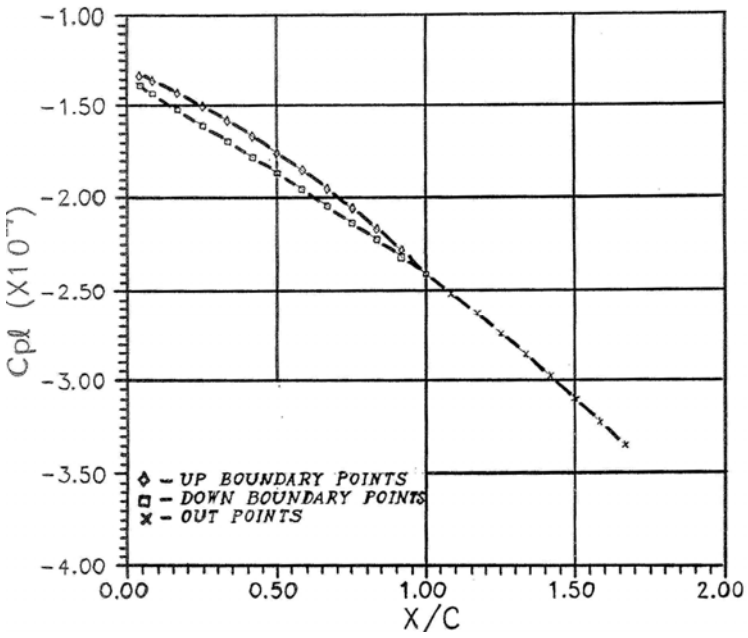

Fig. 9 Pressure distribution on the vertical axis wind turbine of Fig.3, for linear source distribution in the left side of the separating wake and for wind speed 15 m/sec.

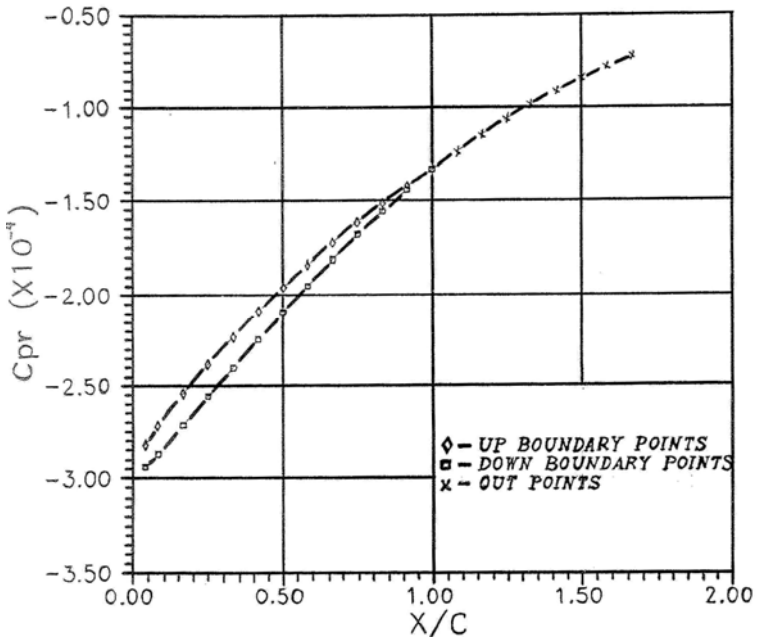

Fig. 10 Pressure distribution on the vertical axis wind turbine of Fig.3, for linear source distribution in the right side of the separating wake and for wind speed 10 m/sec.

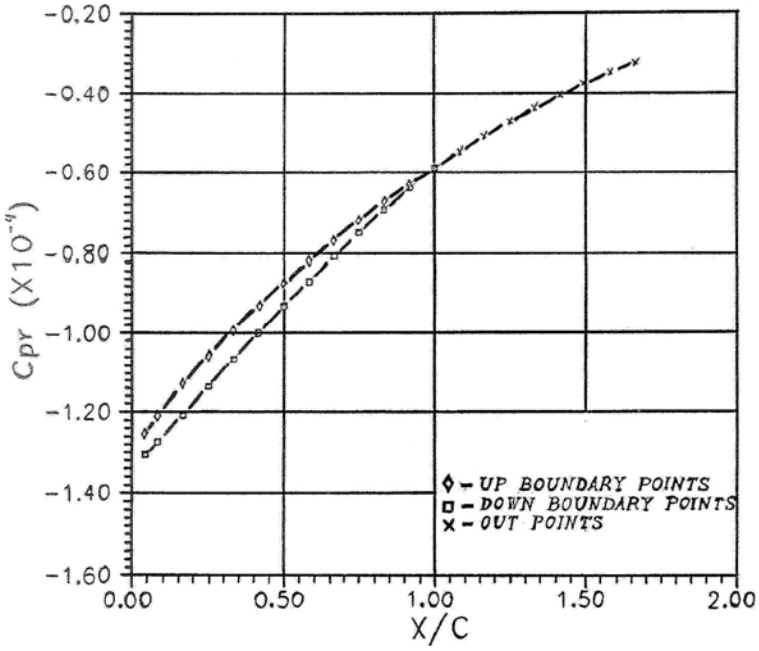

Fig. 11 Pressure distribution on the vertical axis wind turbine of Fig.3, for linear source distribution in the right side of the separating wake and for wind speed 15 m/sec.

By these Figures it is shown that there is a big difference between the two cases, when supposing linear source distribution on the left-hand or right-hand side of the separating wake. The values of C_p for both cases are beginning approximately from -3×10^{-4}, however, for the left-hand distribution are continuously decreasing, while for the right-hand distribution continuously increasing.

Thirdly, by supposing unit vortex distribution, the velocity field on the boundary and around of the airfoil was computed by (2.6.2) for azimuthal angle $\Theta = 90°$. Moreover, the pressure coefficients C_p were calculated through (2.4.4) for several wind velocities U_∞. Figures 12, 13, 14 and 15 show the pressure distribution on the vertical axis wind turbine presented, for wind speed $U_\infty = 10,15,20,25 m/\sec$, respectively.

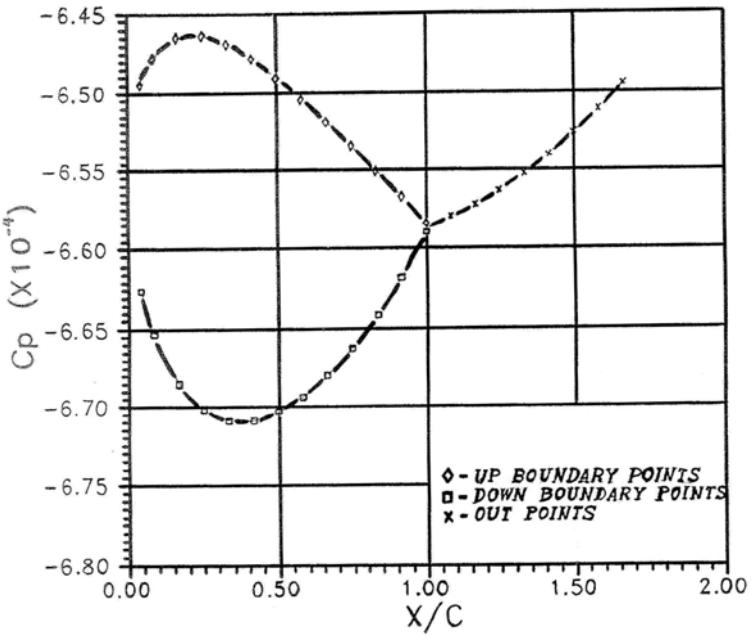

Fig. 12 Pressure distribution on the vertical axis wind turbine of Fig.3, for unit vortex distribution and wind speed 10 m/sec.

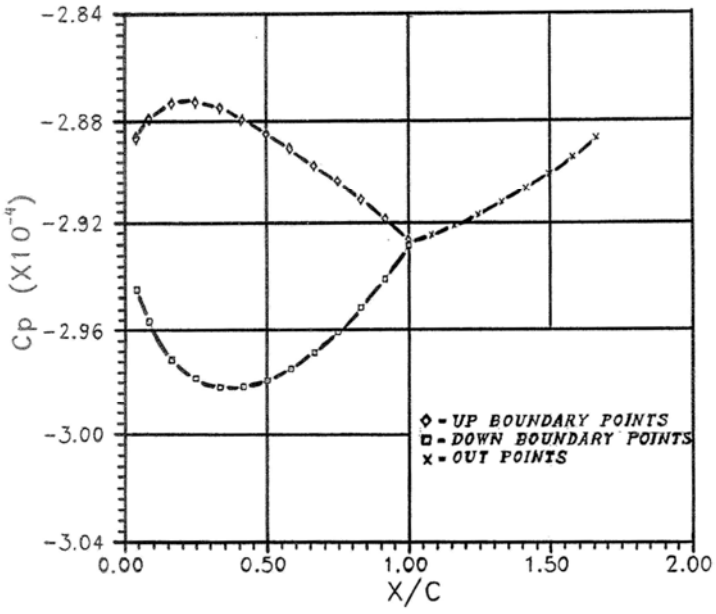

Fig. 13 Pressure distribution on the vertical axis wind turbine of Fig.3, for unit vortex distribution and wind speed 15 m/sec.

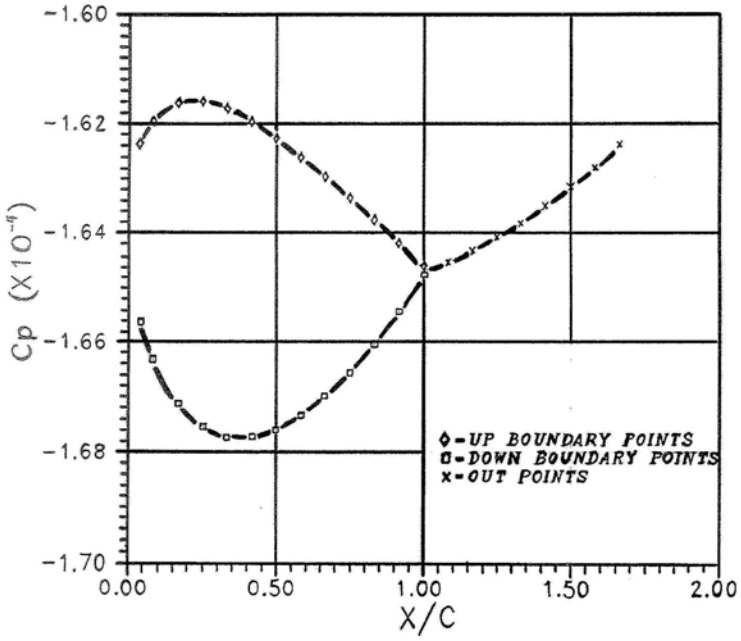

Fig. 14 Pressure distribution on the vertical axis wind turbine of Fig.3, for unit vortex distribution and wind speed 20 m/sec.

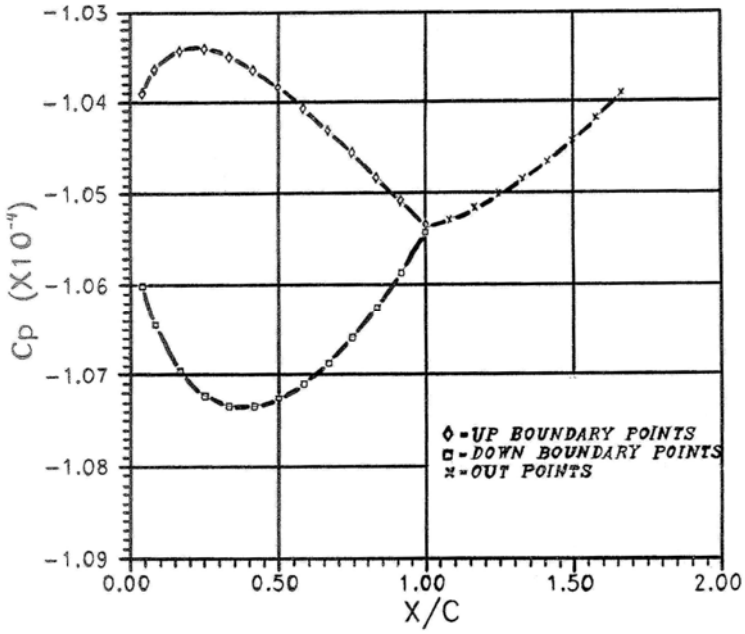

Fig. 15 Pressure distribution on the vertical axis wind turbine of Fig.3, for unit vortex distribution and wind speed 25 m/sec.

By the above Figures it is shown, that for the up boundary points of the airfoil the values of the pressure coefficient are increasing approximately up to $x/c = 0.25$, while then decreasing again up to $x/c = 1$. On the other hand, for the down boundary points the values of the coefficient are decreasing up to $x/c = 0.35$, and then increasing again.

Fourthly, by supposing linear vortex distribution, the velocity field on the boundary and around of the airfoil was computed by (2.7.2) for azimuthal angle $\Theta = 90°$. Also, the pressure coefficients C_p were calculated by (2.4.4) for several wind velocities U_∞ and for angle of attack $a = 20°$. Hence, Figures 16, 17, 18 and 19 show the pressure distribution on the vertical axis wind turbine presented, for wind speed $U_\infty = 10,12,20,25 m/\sec$, respectively.

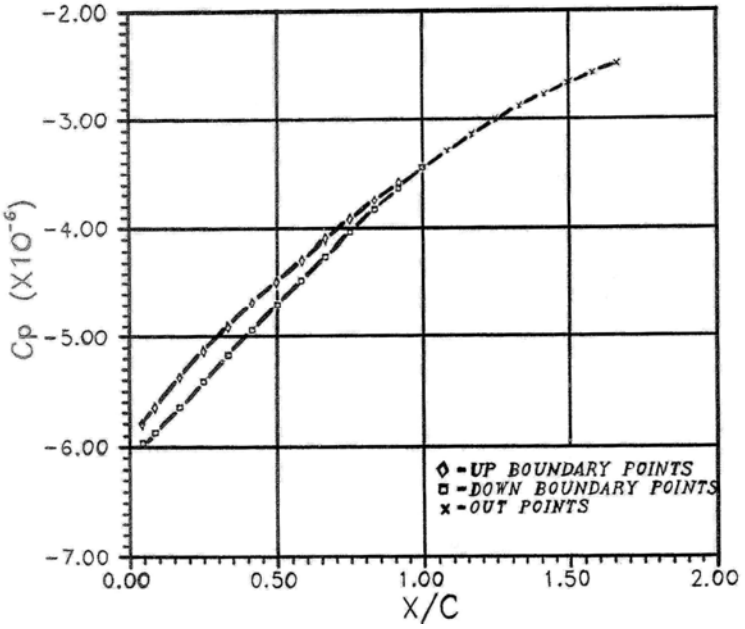

Fig. 16 Pressure distribution on the vertical axis wind turbine of Fig.3, for linear vortex distribution and wind speed 10 m/sec.

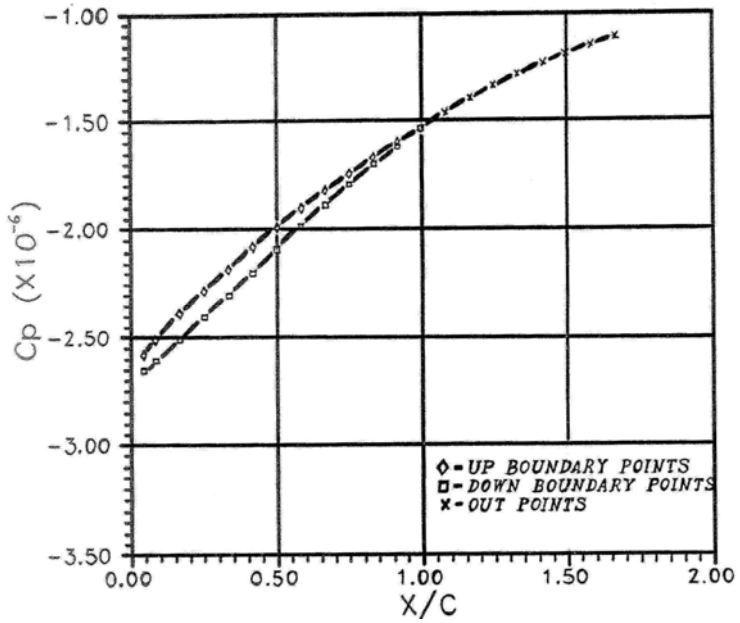

Fig. 17 Pressure distribution on the vertical axis wind turbine of Fig.3, for linear vortex distribution and wind speed 15 m/sec.

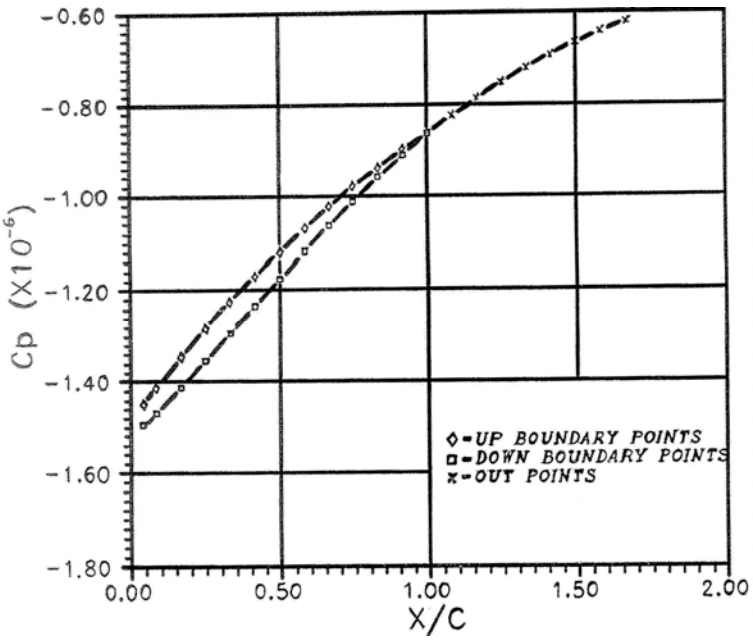

Fig. 18 Pressure distribution on the vertical axis wind turbine of Fig.3, for linear vortex distribution and wind speed 20 m/sec.

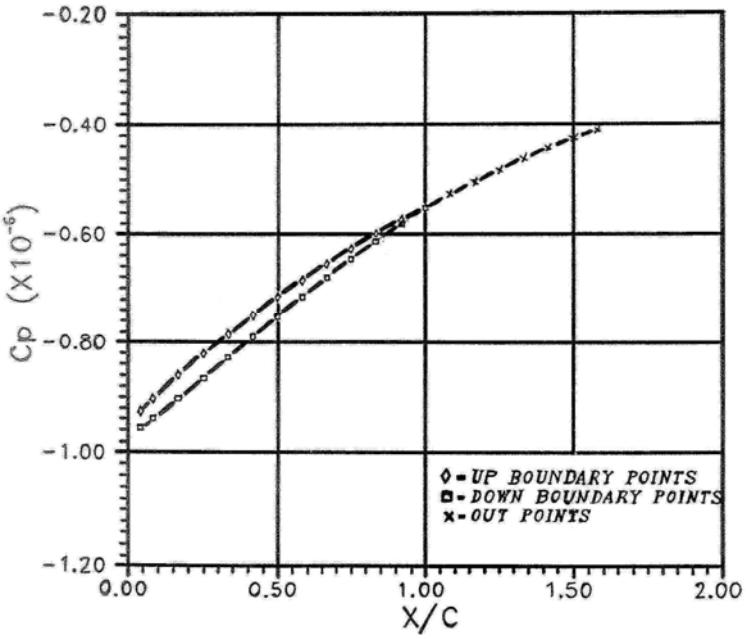

Fig. 19 Pressure distribution on the vertical axis wind turbine of Fig.3, for linear vortex distribution and wind speed 25 m/sec.

By the above Figures, it is shown that the values for both up and down points, are continuously increasing when beginning from x/c= 0 up to x/c =1.

3. Conclusions

As a conclusion to the previous outlined analysis it will be emphasiezed that the proposed method and computer programs will be used for the design of very modern and new generation large vertical axis wind turbines (with diameters up to 200 m and power outputs up to 20 MW).

Also, the Non-linear Singular Integral Computational Method will be used as any easy tool in order to develop the use of unconventional sites, especially in more complex terrains, in regions with lower wind speeds and in regions with very high speeds. This will result by changing the values of the corresponding variables in the computer programs, while up to now the most known data are only experimental, which are difficult to be taken for regions with lower wind speeds, or regions with very high wind speeds.

References

1. *Ladopoulos E.G.,* 'On the numerical solution of the finite – part singular integral equations of the first and the second kind used in fracture mechanics', *Comp. Meth. Appl. Mech. Engng,* ***65*** *(1987), 253 – 266.*
2. *Ladopoulos E.G.,* 'On the solution of the two – dimensional problem of a plane crack of arbitrary shape in an anisotropic material', *J. Engng Fract. Mech.,* ***28*** *(1987), 187 – 195.*
3. *Ladopoulos E.G.,* 'On the numerical evaluation of the singular integral equations used in two and three – dimensional plasticity problems', *Mech. Res. Commun.,* ***14*** *(1987), 263 – 274.*
4. *Ladopoulos E.G.,* 'Singular integral representation of three – dimensional plasticity fracture problem', *Theor. Appl. Fract. Mech.,* ***8*** *(1987), 205 – 211.*
5. *Ladopoulos E.G.,* 'On a new integration rule with the Gegenbauer polynomials for singular integral equations, used in the theory of elasticity', *Ing. Arch.,* ***58*** *(1988), 35 – 46.*
6. *Ladopoulos E.G.,* 'On the numerical evaluation of the general type of finite – part singular integrals and integral equations used in fracture mechanics', *J. Engng. Fract. Mech.,* ***31*** *(1988), 315 – 337.*
7. *Ladopoulos E.G.,* 'The general type of finite – part singular integrals and integral equations with logarithmic singularities used in fracture mechanics', *Acta Mech.,* ***75*** *(1988), 275 – 285.*
8. *Ladopoulos E.G.,* 'On the numerical solution of the multidimensional singular integrals and integral equations used in the theory of linear viscoelasticity', *Int. J. Math. Math. Scien.,* ***11*** *(1988), 561 – 574.*
9. *Ladopoulos E.G.,* 'Singular integral operators method for two – dimensional plasticity problems', *Comp. Struct.,* ***33*** *(1989), 859 – 865.*
10. *Ladopoulos E.G.,* 'Finite – part singular integro – differential equations arising in two – dimensional aerodynamics', *Arch. Mech. ,* ***41*** *(1989), 925 – 936.*
11. *Ladopoulos E.G.,* 'Cubature formulas for singular integral approximations used in three – dimensional elasticity', *Rev. Roum. Sci. Tech., Méc Appl.,* ***34*** *(1989), 377 – 389.*
12. *Ladopoulos E.G.,* 'Relativistic elastic stress analysis for moving frames', Rev. Roum. Sci. Tech., Méch. Appl., ***36*** *(1991), 195 – 209.*
13. *Ladopoulos E.G.,* 'Singular integral operators method for three – dimensional elasto – plastic stress analysis', *Comp. Struct.,* ***38*** *(1991), 1 – 8.*
14. *Ladopoulos E.G.,* 'Singular integral operators method for two – dimensional elasto – plastic stress analysis', *Forsch. Ingen.,* ***57*** *(1991), 152 – 158.*
15. *Ladopoulos E.G.,* 'New aspects for the generalization of the Sokhotski – Plemelj formulae for the solution of finite – part singular integrals used in fracture mechanics', *Int. J. Fract.,* ***54*** *(1992), 317 – 328.*
16. *Ladopoulos E.G.,* 'Singular integral operators method for anisotropic elastic stress analysis', *Comput. Struct.,* ***48*** *(1993), 965 – 973.*
17. *Ladopoulos E.G.,* 'Systems of finite – part singular integral equations in Lp applied to crack problems', *J. Engng. Fract. Mech.,* ***48*** *(1994), 257 – 266.*
18. *Ladopoulos E.G., Zisis V.A. and Kravvaritis D.,* 'Singular integral equations in Hilbert space applied to crack problems', *Theor. Appl. Fract. Mech.,* ***9*** *(1988), 271 – 281.*
19. *Zisis V.A. and Ladopoulos E.G.,* 'Singular integral approximations in Hilbert spaces for elastic stress analysis in a circular ring with curvilinear cracks', *Indus. Math.,* ***39*** *(1989), 113 – 134.*
20. *Zisis V.A. and Ladopoulos E.G.,* 'Two – dimensional singular integral equations exact solutions', *J. Comput. Appl. Math.,* ***31*** *(1990), 227 – 232.*
21. *Ladopoulos E.G., Kravvaritis D. and Zisis V.A. ,* 'Finite – part singular integral representation analysis in Lp of two – dimensional elasticity problems', *J. Engng. Fract. Mech. ,* ***43*** *(1992), 445 – 454.*
22. *Ladopoulos E.G. and Zisis V.A.,* 'Singular integral representation of two – dimensional shear fracture mechanics problem', *Rev. Roum. Sci. Tech., Méc. Appl.,* ***38*** *(1993), 617 – 628.*

23. *Ladopoulos E.G., Zisis V.A. and Kravvaritis D.,* 'Multidimensional singular integral equations in Lp applied to three – dimensional thermoelastoplastic stress analysis', *Comp. Struct., **52** (1994), 781 – 788.*
24. *Ladopoulos E.G.,* 'Non – linear integro – differential equations used in orthotropic spherical shell analysis', *Mech. Res. Commun., **18** (1991), 111 – 119.*
25. *Ladopoulos E.G.,* 'Non-linear integro-differential equations in sandwich plates stress analysis', *Mech. Res. Commun., **21** (1994), 95 – 102.*
26. *Ladopoulos E.G. and Zisis V.A.,* 'Existence and uniqueness for non-linear singular integral equations used in fluid mechanics', *Appl. Math., **42** (1997), 345 – 367.*
27. *Ladopoulos E.G. and Zisis V.A.,* 'Non-linear finite-part singular integral equations arising in two-dimensional fluid mechanics', *Nonlin. Anal., Th. Meth. Appl., **42** (2000) , 277-290.*
28. *Ladopoulos E.G.,* 'Non-linear singular integral representation for unsteady inviscid flowfields of 2-D airfoils', *Mech. Res. Commun., **22** (1995), 25 – 34.*
29. *Ladopoulos E.G.* 'Non-linear singular integral representation analysis for inviscid flowfields of unsteady airfoils', *Int. J. Non-Lin. Mech., **32** (1997), 377 – 384.*
30. *Ladopoulos E.G. and Zisis V.A.,* 'Non-linear singular integral approximations in Banach spaces', *Nonlin. Anal., Theor. Math. Appl., **26** (1996), 1293 – 1299.*
31. *Smith A.M.O. and Hess J.L.,* 'Calculation of the non-lifting potential flow about arbitrary three dimensional bodies', *Douglas Report E.S. 40622 (1967).*
32. *Djojodihardjo R.H. and Windnall S.E.,* 'A numerical method for the calculation of non-linear unsteady lifting potential flow problems', *AIAA J., **7** (1969), 2001-2009.*
33. *Robert P.E.and Saaris G.R., 'Review and evaluation of a three-dimensional lifting potential flow computational method for arbitrary configurations',* Boeing Co*,.1972.*
34. *Summa J.M.,* 'Potential flow about impulsively started rotors', *J.Aircraft, **13**(1976), 317-319.*
35. *Sarpkaya T. and.Schoaff R.L,* 'Inviscid model of two-dimensional vortex shedding by a circular cylinder', *AIAA J., **17**(1979), 1193-1200.*
36. *Bristow D.R.,* 'Development of panel methods for subsonic analysis and design', *NASA CR - 3234 (1980).*
37. *Bristow D.R. and Hawk J.D.,* 'Subsonic panel method for the efficient analysis of multiple geometry perturbations', *NASA CR-3258 (1982).*
38. *Lewis R.I.,* 'Surface vorticity modeling of separated flows from two-dimensional bluff bodies of arbitrary shape', *J. Mech. Engng Sci,. **21**(1981), 1-12.*
39. *Ham N.D.,* 'Aerodynamic loading on a two-dimensional airfoil during dynamic stall', *AIAA J, **6**(1968), 1927-1934.*
40. *Deffenbaugh F.D. and Marschall F.J.,* 'Time development of the flow about an impulsively started cylinder', *AIAA J.,**14**(1976), 908-913.*
41. *Kiya M. and Arie M.,* 'A contribution to an inviscid vortex-shedding model for an inclined flat plate in uniform flow', *J. Fluid Mech., **82**(1977), 223-240.*
42. *Sarpkaya T. and Kline H.K.,* 'Impulsively-started flow about four types of bluff body', *J. Fluid Engng, **104**(1982), 207-213.*
43. *Singleton R.E. and .Nash J.F,* 'Method for calculating unsteady turbulent boundary layers in two- and three-dimensional flows', *AIAA J., **12**(1974), 590-595.*
44. *Nash J.F., Carr L.W. and Singleton R.E.,* 'Unsteady turbulent boundary layers in two-dimensional incompressible flow', *AIAA J, **13**(1975), 176-183.*
45. *Lyrio A.A., Ferzinger J.H. and Kline S.J.,* 'An integral method for the computation of steady and unsteady turbulent boundary layer flows including the transitory stall regine in diffusers', *Stanford University Report, PD-23 (1981).*
46. *Kim J., Kline S.J. and Johnston J.P.,*'Investigation of separation and reattachment of a turbulent shear layer: flow over a backward-facing step', *J. Fluid Engng, **102**(1982), 392-398.*
47. *McCroskey W.J. and Pucci S.I.,* 'Viscous-inviscid interaction on oscillating airfoil in subsonic flow', *AIAA J., **20**(1982), 167-174.*
48. *Muraca R.J., Stephens M.V. and Dagenhart J.R.,* 'Theoretical performance of cross-wind axis turbines for a catenacy vertical axis configuration', *NASA TMX-72662 (1975).*

49. *Strickland J.H.,* 'The Darrieus turbine: a performance prediction model using multiple streamtubes', *SAND 75-0431 (1975).*

50. *Shankar P.N.,* 'The Darrieus turbine: a performance of a class of vertical shaft windmills', *Proc. R. Soc. Lond.,* ***A349****(1976), 35-51.*

51. *Wilson R.E., Lissaman P.B.S. and Walker S.N.,* 'Aerodynamic performance of wind turbines', *Oregon State University, NTIS PB-259089 (1976).*

52. *Paraschivoiu I.,* 'Aerodynamic loads and performance of the Darrieus rotor', *J. Energy,* ***6****(1982), 406-412.*

53. *Paraschivoiu I., Delclaux F., Fraunie P. and Beguier C.,* 'Aerodynamic analysis of the Darrieus rotor including secondary effects', *J. Energy,* ***7****(1983), 416-422.*

54. *Loth J.L. and McCay H.,* 'Optimization of Darrieus turbines with an upwind and downwind momentum model', *J. Energy* ***7****(1983), 313-318.*

55. *Fanucci J.B. and Walters R.E.,* 'Innovative wind machines, the theoretical performance of a VAWT', *Proc. VAWT Technic. Work, SAND 76-5586 (1976).*

56. *Strickland J.H., Webster B.T.and Nguyen T.,* 'A vortex model of the Darrieus turbine: an analytical and experimental study', *J. Fluid Engng, Trans. ASME,* ***101****(1979), 501-505.*

57. *Strickland J.H., Webster B.T. and Nguyen T.,* 'A vortex model of the Darrieus turbine: an analytical and experimental study', *SAND-79-7058 (1980).*

58. *Lamb H., 'Hydrodynamics',* Dover, New York*, 1932.*

59. *Karamcheti K., 'Principles of Ideal-Fluid Aerodynamics',* Wiley, New York, *1966.*